Advantage of delayed whole-body FDG-PET imaging for tumour detection

Kazuo Kubota[1], Masatoshi Itoh[3], Kaoru Ozaki[3], Shuichi Ono[1], Manabu Tashiro[3], Keiichiro Yamaguchi[3], Takashi Akaizawa[1], Kenji Yamada[2], Hiroshi Fukuda[1]

[1] Department of Nuclear Medicine and Radiology, Institute of Development, Aging and Cancer, Tohoku University, 4-1 Seiryocho, Aobaku, Sendai 980-8575, Japan
[2] Sendai Kosei Hospital, Japan
[3] Cyclotron and Radioisotope Center, Tohoku University, Japan

Received 23 January and in revised form 13 March 2001 / Published online: 8 May 2001

Abstract. Delayed imaging that coincides with the highest uptake of fluorine-18 fluorodeoxyglucose (FDG) by tumour may be advantageous in oncological positron emission tomography (PET), where delineation of metastasis from normal tissue background is important. In order to identify the better imaging protocol for tumour detection, whole-body FDG-PET images acquired at 1 h and 2 h after injection were evaluated in 22 subjects, with a post-injection transmission scan at 90 min for attenuation correction. After visual interpretation, tumour uptake [tumour standardised uptake ratio (SUR)], normal tissue uptake (normal SUR) and tumour to background contrast (tumour SUR/normal tissue SUR) were evaluated in the images acquired at 1 h and at 2 h. Most malignant lesions, including primary lung cancer, metastatic mediastinal lymph nodes and lymphoma lesions, showed higher FDG uptake at 2 h than at 1 h. By contrast, benign lesions, with the exception of sarcoidosis, showed lower uptake of FDG at 2 h than at 1 h. Among normal tissues, the kidney, liver, mediastinum, lung, upper abdomen and left abdomen showed significant falls in FDG uptake from 1 h to 2 h. The lower abdomen, right abdomen and muscles (shoulder and thigh) showed no significant changes. Consequently, malignant lesions of the lung, mediastinum and upper abdomen showed significant increases in tumour to background contrast from 1 to 2 h. Three lesions (two lung cancers and a malignant lymphoma) that were equivocal on 1-h images became evident on 2-h images, changing the results of interpretation. All other malignant lesions were detected on 1-h images, but were clearer, with higher contrast, on 2-h images. Lesion-based sensitivity was improved from 92% (49/53) to 98% (52/53), and patient-based sensitivity from 78% (14/18) to 94% (17/18). It is concluded that delayed whole-body FDG-PET imaging is a better and more reliable imaging protocol for tumour detection.

Keywords: Fluorine-18 fluorodeoxyglucose – Positron emission tomography – Tumour detection – Delayed imaging – Lung cancer

Eur J Nucl Med (2001) 28:696–703
DOI 10.1007/s002590100537

Kazuo Kubota (✉)
Department of Nuclear Medicine and Radiology,
Institute of Development, Aging and Cancer, Tohoku University,
4-1 Seiryocho, Aobaku, Sendai 980-8575, Japan
e-mail: kkubota@idac.tohoku.ac.jp
Tel.: +81-22-7178559, Fax: +81-22-7178560

Introduction

Enhanced glycolysis is a unique characteristic of cancer cells and has been studied in human cancers with positron emission tomography using fluorine-18 fluorodeoxyglucose (FDG-PET) [1]. The clinical usefulness of FDG-PET for tumour detection and staging has been well established in a variety of malignant diseases such as lung cancer [2, 3], malignant lymphoma [4, 5] and breast cancer [6, 7]. In most of these FDG-PET studies, imaging was performed at 50–60 min after FDG injection. The study protocol with FDG was originally established in studies measuring cerebral glucose metabolism [8], and was subsequently applied to oncology [9]. Because quantitative measurement correlates well with qualitative interpretation [10], the simple imaging method at 50–60 min after injection of FDG without blood sampling became popular. Recently, even images without attenuation correction have been widely used, and this method has been found to correlate well with image acquisition after attenuation correction [11].

With respect to the timing of imaging of tumours when using FDG, several validation studies have been

reported [12, 13]. Our animal studies showed that the pattern of FDG uptake by cancer cells was different from that of normal cells, and suggested that dynamic PET might be helpful for establishing the correct diagnosis [12]. Furthermore, Lowe et al. [13] performed dynamic PET studies and reported that lung cancer FDG uptake reached a peak at 2 h or even later; however, the best separation from benign tumours was at 50–60 min. Quantitative studies using a three-compartment model showed that the calculated peak of FDG uptake by lung cancer occurred at 4–6 h [14]. Recent oncological whole-body PET studies have usually been designed with the aim of tumour staging, for which purpose delineation of metastasis from normal tissue background is most important. Delaying imaging until the tumour uptake becomes highest may be advantageous. For example, favourable results have been reported using whole-body PET imaging at 90 min post injection (p.i.) for the detection of a variety of tumours [15, 16]. In another study of PET for breast cancer, tumour contrast was reported to be better at 3 h than at 1.5 h p.i. [17]. However, to our knowledge, the effects of timing of imaging on the contrast in FDG uptake by tumour and normal tissue have never been evaluated in whole-body imaging. In this study, we compared images acquired 1 h and 2 h after injection in order to determine the best whole-body FDG-PET imaging protocol for tumour detection.

Materials and methods

Subjects. A total of 22 subjects (11 with lung cancers, 1 with benign mesothelioma, 1 with sarcoidosis, 4 with malignant lymphomas, 1 with multiple myeloma, 1 with liver carcinoid tumour, 2 who had undergone surgery for colon and breast cancers and were suspected of recurrence, and 1 normal healthy subject) were studied with FDG-PET. A total of 60 lesions were identified in whole-body images of these patients. All patients had a complete radiological diagnostic work-up before or after PET studies. Histological confirmation of the diagnosis was performed in all patients. Furthermore, PET images were compared with conventional imaging studies and clinical observations. Eight patients, including six with lung cancers, one with localised mesothelioma and one with malignant lymphoma, underwent surgery for removal of the malignant tumours. Results of surgical pathology were compared with those of PET in these patients. The study was approved by the Ethics Committee for Clinical Research of Tohoku University, and written informed consent was obtained from all subjects.

PET imaging. FDG was prepared using an automated synthesis system, and quality assurance tests were performed as described previously [18]. Blood glucose level was measured after fasting for more than 5 h. Thereafter a bolus injection of a mean dose of 100 MBq of FDG was administered while the subject sat in a comfortable chair in a quiet room. During the time between injection and scanning, the subject was asked to remain still to minimise FDG consumption of the striated muscles. All patients were asked to void just before scanning. Whole-body PET scans were performed using a dedicated PET scanner (Shimadz SET2400 W, Kyoto, Japan: axial resolution 3.9 mm FWHM, field of view z-axis 20 cm) with the multiple bed-position technique. Three-dimensional (3D) data acquisition without septa, and image reconstruction with scatter correction using a super computer system were performed as described previously [19]. The sensitivity in 3D acquisition mode is eight times as high as that in the 2D mode. This allowed lowering of the injection dose and shortening of the scanning time while at the same time preserving the quality of the acquired images. Sixty minutes after injection, the first whole-body scan with 3 min emission scan per bed position of 6–7 increments was started (total scanning time: 3×6–7 min = 18–21 min), providing a whole-body scan from the mid thigh to the vertex. This was followed by a post-injection transmission scan with an external source (370 MBq of $^{68}Ge/^{68}Ga$). Patients were asked not to move while on the scanning table, and a second whole-body scan with 4 min emission scan per bed position was started from 120 min after injection. Two emission scans shared a transmission scan for attenuation correction. The total occupancy time of the PET scanner in this protocol was about 90 min per patient. No significant artefacts due to body movement during transmission and emission scans were observed.

Data analysis. PET images were reconstructed using measured attenuation correction, dead-time correction and decay correction to the beginning of each scan. All images were initially evaluated visually. Foci of intense uptake exceeding the uptake of the surrounding normal structures and of nodular appearance were considered malignant. PET images were analysed and compared with conventional images and histological diagnosis retrospectively. For the comparison of images acquired at 1 h and 2 h, the original axial slices were re-sliced to coronal images with 16 mm thickness and images acquired at 1 h and 2 h were displayed simultaneously using the same windowing and levelling. Regions of interests (ROIs) were placed on all tumour lesions and normal tissues. Tumour ROIs included the highest radioactivity point. Normal tissue ROIs (Fig. 1), except kidneys, were marked on two sequential coronal images just anterior to the level of the vertebral body and averaged. Muscle ROI data of both shoulders and thighs and ROI data of both lungs were averaged. ROIs were marked on the liver, mediastinum (avoiding the myocardium), upper abdomen (corresponding to the para-aortic area), lower abdomen (para-aorta), right abdomen and left abdomen. ROIs in the abdomen were marked avoiding intense activity in the kidney, ureter and bladder. ROIs in the abdomen in some patients did, however, include intestinal activity. A part of the normal pancreas seemed to be included in the ROI of the upper abdomen, but this was not seen in our subjects. ROIs were also marked on both kidneys in separate coronal images including the largest section of the kidneys. All ROI data were decay corrected to the injection time. The standardised uptake ratio (SUR) was calculated according to the following formula [20].

$$\mathrm{SUR} = \frac{\mathrm{ROIdata\ (cps/ml)} \times \mathrm{Bodyweight}}{\mathrm{calibrationfactor\ (cps/mCi/ml)} \times \mathrm{injecteddose\ (mCi)}}$$

All data were expressed as mean±SD. Differences in FDG uptake between 1-h and 2-h images, as reflected by SUR or SUR/background values, were examined for statistical significance using the Wilcoxon's signed-rank test or paired *t* test. A *P* value less than 0.05 was taken to denote a statistically significant difference.

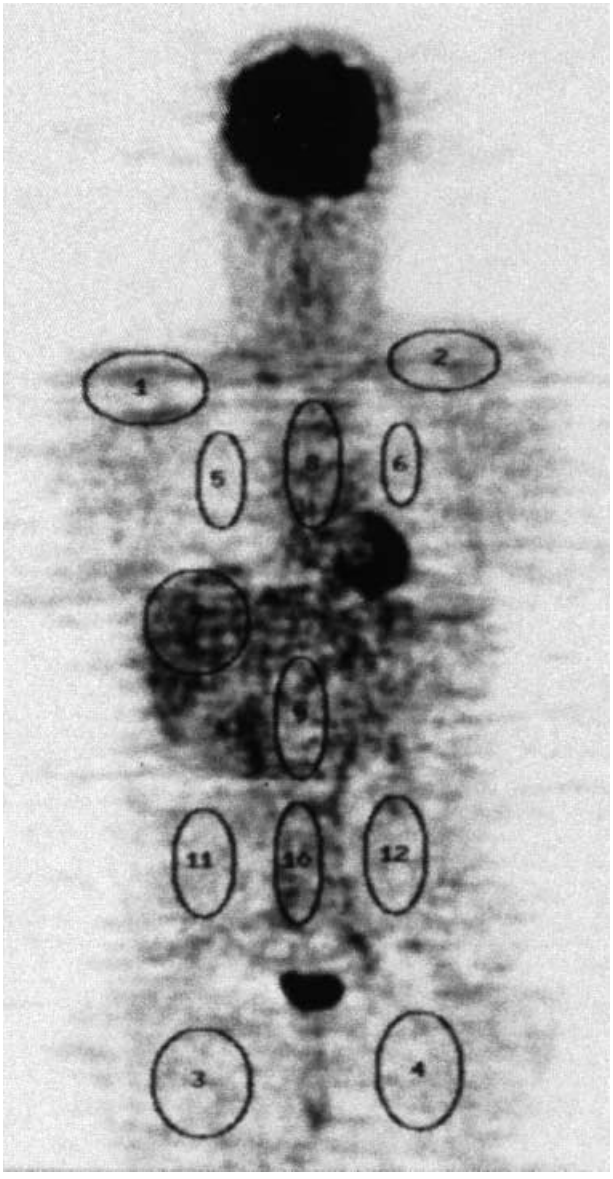

Fig. 1. Illustration of regions of interest (ROIs) on normal tissue in whole-body FDG-PET imaging. Muscle (shoulder and thigh), lung, liver, mediastinum, upper abdomen, lower abdomen, and right and left abdomen are marked on two sequential coronal images just anterior to the level of the vertebral bodies and averaged. Kidneys are marked on separate coronal images (not shown) including the largest section of kidneys

Results

Two tumours that were equivocal on 1-h images in two patients, a solitary nodule at the lung base and a solitary enlarged lymph node in the upper abdomen, were evident on the 2-h images (Fig. 2). These were pathologically diagnosed as lung cancer and malignant lymphoma, respectively, after the PET studies. Similarly, a mediastinal lymph node metastasis in a patient with lung cancer that was equivocal at 1 h became clearly evident at 2 h. Multiple liver tumours identified by contrast-enhanced computed tomography (CT) were not seen on 1-h or 2-h images; they were later diagnosed as carcinoid by biopsy examination. All other malignant lesions could be seen on the 1-h images, but were better seen, with higher contrast, on the 2-h images. The lesion-based sensitivity of the 1-h images was 92% (49/53), while the patient-based sensitivity of 1-h images was 78% (14/18). The corresponding figures for the 2-h images were better, at 98% (52/53) and 94% (17/18), respectively (Table 1). For diagnostic purposes, images of tumour lesions at 2 h were of better quality than those acquired at 1 h in all patients.

Data on tumour FDG uptake (SUR at 1 h and 2 h) are summarised in Table 2. Most malignant lesions, including primary lung cancer (Fig. 3), mediastinal metastatic lymph nodes (Fig. 4) and lymphoma lesions (Fig. 5), showed higher FDG uptake at 2 h than at 1 h. The increase in FDG uptake from 1 h to 2 h was statistically significant in primary tumours of lung cancer and in neck and axillary lesions of malignant lymphoma (Table 2). Bone lesions of multiple myeloma showed lower uptake at 2 h than at 1 h.

Among benign lesions, sarcoidosis showed higher FDG uptake at 2 h, while benign mesothelioma showed lower FDG uptake at 2 h. A supraclavicular lesion seen postoperatively in a patient with breast cancer showed lower uptake on the 2-h image than on the 1-h image. It was later confirmed to be a post-radiotherapy inflammatory lesion. No lesions displaying FDG uptake were seen postoperatively in a patient with colon cancer or in the normal subject.

Normal tissue FDG uptake (SUR at 1 h and 2 h) is summarised in Table 3. Most normal tissues showed a lower FDG uptake at 2 h than at 1 h. On the other hand, uptake by the muscles, the lower abdomen and the right

Table 1. Detection of malignant lesions (visual interpretation) on PET images at 1 h and 2 h after injection

	Images at 1 h		Images at 2 h	
	Positive	Negative	Positive	Negative
No. of patients	14	4	17	1
Sensitivity	78% (14/18)		94% (17/18)	
No. of lesions	49	4	52	1
Sensitivity	92% (49/53)		98% (52/53)	

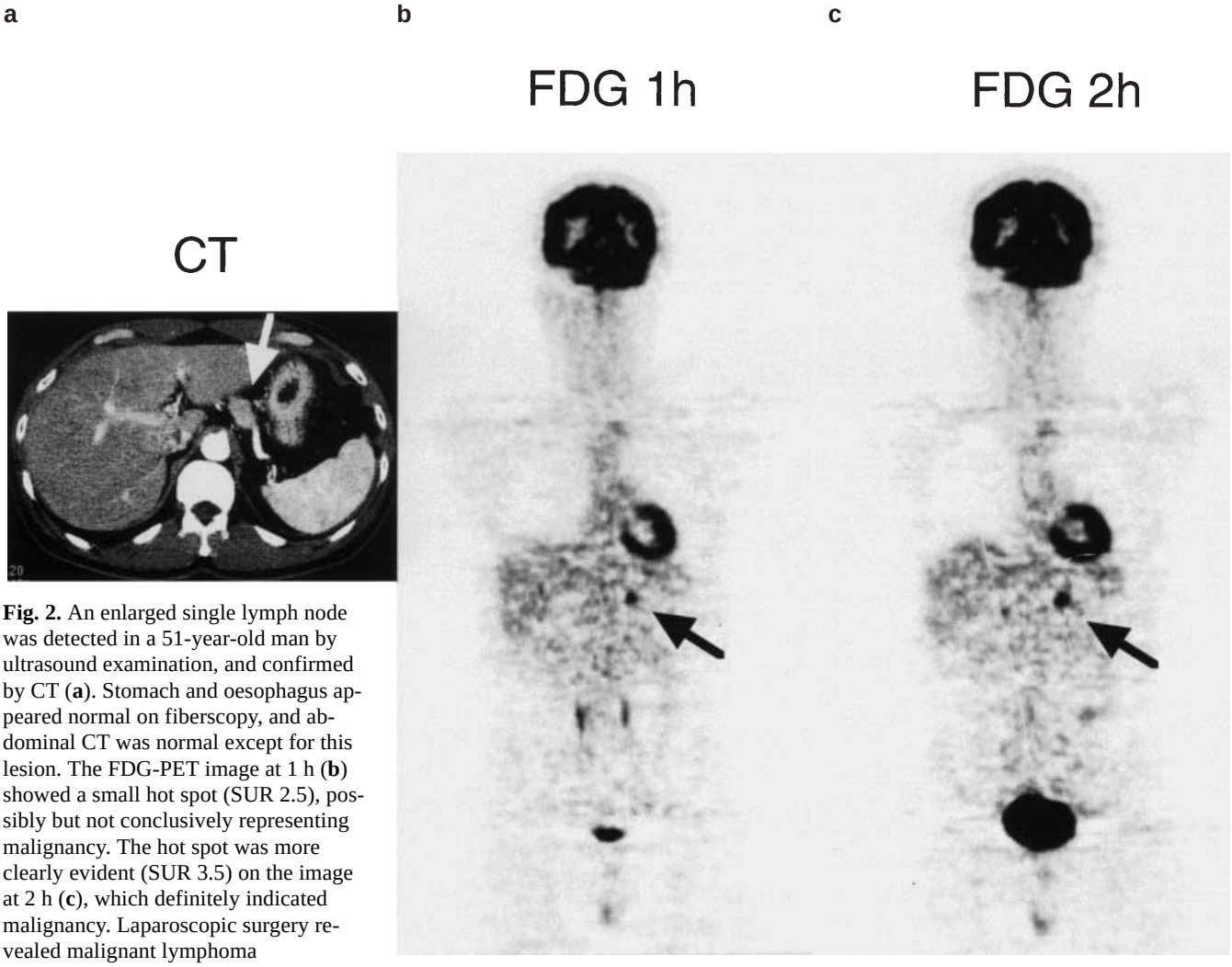

Fig. 2. An enlarged single lymph node was detected in a 51-year-old man by ultrasound examination, and confirmed by CT (**a**). Stomach and oesophagus appeared normal on fiberscopy, and abdominal CT was normal except for this lesion. The FDG-PET image at 1 h (**b**) showed a small hot spot (SUR 2.5), possibly but not conclusively representing malignancy. The hot spot was more clearly evident (SUR 3.5) on the image at 2 h (**c**), which definitely indicated malignancy. Laparoscopic surgery revealed malignant lymphoma

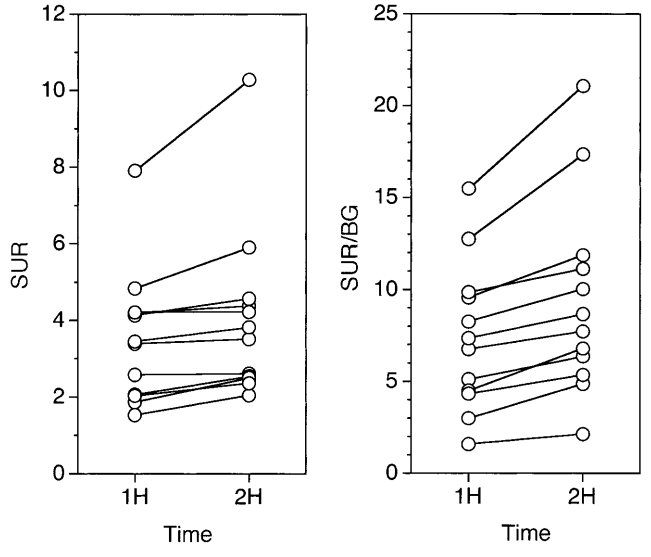

Fig. 3. Comparison of FDG uptake by primary lung cancer at 1 h and 2 h, evaluated by tumour SUR (*left panel*) and by tumour SUR to lung SUR (background) contrast (*right panel*). A significant increase in SUR (P<0.005) was noted from 1 h to 2 h. Note the larger increase in SUR/BG (P<0.005)

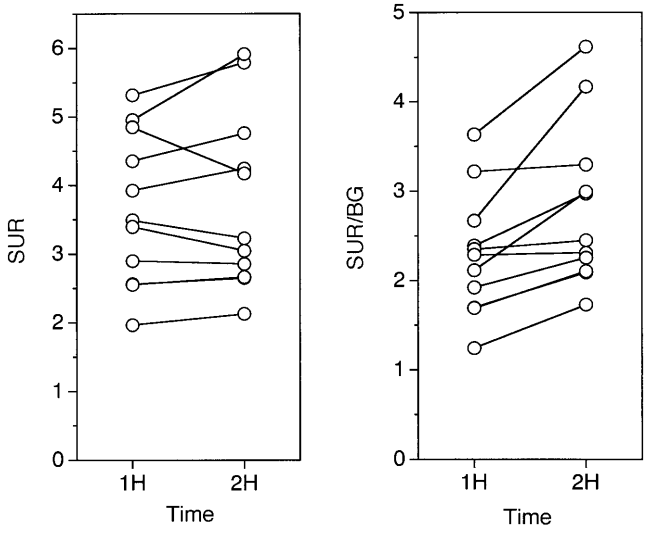

Fig. 4. Comparison of FDG uptake by metastatic mediastinal lymph nodes of lung cancer at 1 h and 2 h, evaluated by tumour SUR (*left panel*) and by tumour SUR to mediastinal SUR (background) contrast (*right panel*). There was no significant change in SUR from 1 h to 2 h, but a significant change in SUR/BG was observed (P<0.005)

Table 2. Tumour uptake (SUR) and tumour to background contrast (SUR/BG) in whole-body FDG-PET at 1 h and 2 h post injection

Disease (no. of pts.) and lesion (*n*)	FDG uptake (SUR)				FDG uptake contrast (SUR/BG)[b]			
	1 h	2 h	% change[a]	*P* value	1 h	2 h	% change	*P* value*
Malignant								
Lung cancer (11 pts.)								
Neck LN (*n*=2)	2.131±0.309	2.438±0.973	+14.4		2.611±0.379	3.143±1.255	+20.4	
Primary + lung mets. (*n*=12)	3.514±1.763	4.061±2.269	+15.6	*P*<0.005	7.374±4.069	9.443±5.378	+28.1	*P*<0.005
Mediastinal LN mets. (*n*=11)	3.660±1.111	3.769±1.298	+3.0		2.292±0.692	2.817±0.909	+22.9	p<0.005
Colon tumour (*n*=1)	2.497	2.826	+13.2		2.874	3.920	+36.4	
Lymphoma (4 pts.)								
Lung lesions (*n*=2)	6.518±4.601	7.168±5.428	+10.0		11.019±7.778	15.581±1.799	+41.4	
Neck and axillary LN (*n*=10)	3.765±2.039	4.021±2.297	+6.8	*P*<0.025	6.061±2.434	6.308±2.671	+4.1	
Mediastinal LN (*n*=3)	6.393±2.901	6.992±2.183	+9.4		4.123±2.152	5.496±2.402	+33.3	
Upper abdominal LN (*n*=5)	4.117±1.769	4.678±2.660	+13.6		2.993±1.349	3.810±1.913	+27.3	*P*<0.05
Lower abdominal LN (*n*=1)	3.904	5.280	+35.2		3.020	4.414	+46.2	
Left abdominal LN (*n*=3)	4.344±2.404	4.753±1.588	+9.4		4.165±1.975	5.149+1.277	+23.6	
Multiple myeloma (1 pt.)								
Bone (*n*=1)	3.427	3.362	–1.9		3.796	3.288	–13.3	
Upper abdominal tumour (*n*=1)	10.538	13.126	+24.6		5.692	7.703	+35.3	
Liver carcinoid tumour (1 pt.)	1.819	1.619	–11.0		1	1	0	
Benign								
Sarcoidosis (1 pt.)								
Neck LN (*n*=1)	1.069	1.816	+69.9		2.550	3.670	+43.9	
Mediastinal LN (*n*=3)	2.596±0.761	3.004±0.762	+15.7		2.318±0.680	3.286±0.834	+41.7	
Upper abdominal LN (*n*=1)	2.382	2.307	–3.1		2.051	2.381	+16.1	
Localised mesothelioma (1 pt.)	0.944	0.899	–4.8		1.196	1.196	0	
Breast postop., post radiation[c] (1 pt.)	2.312	2.033	–12.1		2.917	2.597	–11.0	

A patient with colon cancer had no lesion after surgery. A total of 60 lesions in 21 patients and a normal volunteer were studied.
All data are mean and SD of each lesion
**P* value: comparison of uptake at 1 h and 2 h by Wilcoxon's signed rank test

[a] (SUR 2 h–SUR 1 h)/SUR 1 h×100 was calculated for each lesion, then averaged
[b] SUR of lesion/SUR of background was calculated for each lesion, then averaged
[c] This was an inflammatory lesion post radiotherapy

Table 3. Normal tissue FDG uptake (SUR) in whole-body PET 1 h and 2 h post injection (n=22)

Tissue	1 h[a]	2 h[a]	% change[b]	P value
Muscle	0.792±0.145	0.791±0.145	0.243±7.137	NS
Lung	0.521±0.183	0.466±0.193	–11.637±7.775	P<0.005
Liver	1.743±0.250	1.473±0.257	–15.703±4.824	P<0.002
Mediastinum	1.558±0.250	1.313±0.196	–15.415±6.295	P<0.001
Upper abdomen	1.337±0.159	1.183±0.161	–11.444±6.612	P<0.005
Lower abdomen	1.180±0.140	1.174±0.140	–0.410±5.728	NS
Right abdomen	0.930±0.137	0.906±0.134	–2.249±7.801	NS
Left abdomen	0.923±0.141	0.869±0.132	–5.245±10.835	P<0.025
Kidney, rt. (n=21)	2.199±0.467	1.680±0.361	–22.613±12.291	P<0.005
Kidney, lt. (n=22)	2.151±0.579	1.613±0.258	–22.441±12.790	P<0.001

*P value: comparison of uptake at 1 h and 2 h by Wilcoxon's signed rank test
[a] Mean and SD of individual SUR
[b] (SUR 2 h–SUR 1 h)/SUR 1 h×100 was calculated for individual data, then averaged

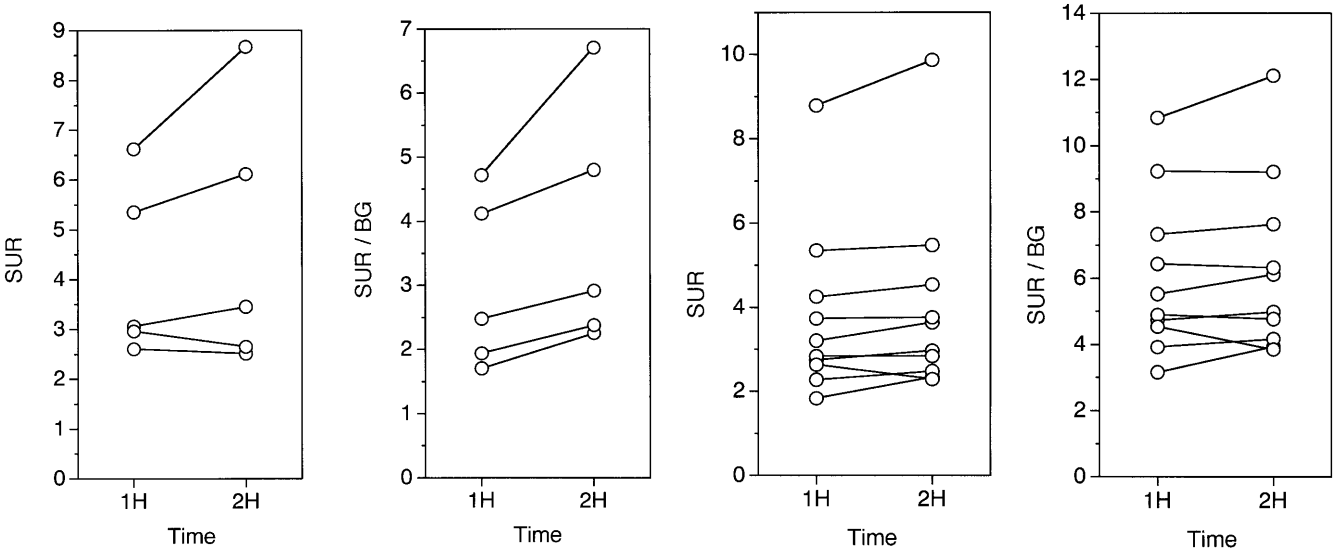

Fig. 5. Comparison of FDG uptake by upper abdominal lesions of malignant lymphoma at 1 h and 2 h, evaluated by tumour SUR (*left panel*) and by tumour SUR to upper abdominal SUR (background) contrast (*right panel*). There was no significant change in SUR from 1 h to 2 h, but a significant change in SUR/BG was observed (P<0.05)

Fig. 6. Comparison of FDG uptake by neck and axillary lesions of malignant lymphoma at 1 h and 2 h, evaluated by tumour SUR (*left panel*) and by tumour SUR to muscle SUR (background) contrast (*right panel*). There was a significant increase in SUR (P<0.05) from 1 h to 2 h, but no significant change in SUR/BG

abdomen was not significantly different at 2 h. The activity of the bladder and visible ureter was excluded from the ROI of the lower abdomen; however, some of the scatter contamination from these areas seemed to affect the ROI count of the lower abdomen, especially in the 2-h images. Because in this study patients were asked to lie on the scanning bed between the 1- and 2-h scans, bladder activity on the 2-h scan was higher than that on the 1-h scan.

We also compared the tumour to background contrast at 1 h and 2 h (Table 2). Malignant lesions, especially those in the lung (Fig. 3), mediastinum (Fig. 4) and upper abdomen (Fig. 5), showed large significant increases in tumour to background contrast at 2 h. On the other hand, lymphoma lesions in the neck and axillae showed no significant changes in tumour to background contrast (Fig. 6), because the background muscle showed a stable or slight increase in FDG uptake from 1 h to 2 h. The percent change in tumour to background contrast was larger than that in tumour SUR in most tumour lesions.

Discussion

The major findings in this study were as follows: (1) Most malignant tumours showed a higher FDG uptake at 2 h than at 1 h. (2) Most normal tissues showed a lower FDG uptake at 2 h than at 1 h. (3) Consequently, tumour to background contrast was enhanced at 2 h, and the sensitivity was improved. Delayed imaging changed the uptake by three malignant lesions from being equivocal at 1 h to being evidently elevated at 2 h. Image interpretation changed in these three patients. These results clearly suggest significant advantages of delayed FDG-PET im-

aging at 2 h for cancer detection. However, delayed imaging at 2 h may not be helpful for differentiating malignant lesions from active inflammation such as sarcoidosis. In addition, the stable uptake by muscles seems to hinder the delineation of some lesions, such as lymph nodes in the axilla and neck, even on 2-h images.

Several studies have shown the advantages of delayed imaging with FDG. Using FDG-PET for breast cancer, it was shown that the tumour to non-tumour ratio was significantly higher in 3-h images than in 1.5-h images. Furthermore, lesion detectability increased from 83% at 1.5 h to 93% at 3 h [17]. Delayed scan was also useful for the diagnosis of pancreatic cancer; most pancreatic cancers showed a higher FDG uptake at 2 h than at 1 h, and several tumours showed even higher uptake at 3 h [21]. Lowe et al. [13] applied dynamic FDG-PET for the study of lung cancers up to 2.5 h after injection, and found that most tumours showed peak FDG uptake at around 2–2.5 h. Hamberg et al. [14] examined dynamic FDG-PET of lung cancer until 1.5 h with blood sampling and full quantification. They extrapolated their data and showed that tumour uptake reached a peak level at around 4–6 h. Although direct comparisons of 1-h and 2-h images of whole-body FDG-PET for lung cancer and malignant lymphoma have not yet been reported, previous studies seem to be consistent with our results.

Previous studies have focussed on changes in FDG uptake by the tumour itself. In the clinical setting of whole-body PET imaging for the purpose of oncological diagnosis, the tumour to background contrast is an important factor in the detection of metastatic lesions. In this study, we systemically evaluated normal tissue uptake in whole-body images for the first time, and found that the tumour to background contrast dramatically improved at 2 h, relative to that at 1 h, in lung, mediastinal and upper abdominal lesions but not in neck and axillary lesions. Such improvement is most likely to be due to the marked decrease in uptake by normal lung, mediastinum, liver, upper abdomen and kidney. In particular, the low FDG uptake in the kidney and liver on 2-h images facilitates the evaluation of lesions in the abdomen. When images at 2 h were obtained just after voiding, a better tumour to background contrast was obtained in the lower abdomen. Because in our research protocol, 2-h images were obtained about 1 h after voiding, the high radioactivity in the bladder interfered with accurate evaluation of lesions in the lower abdomen. In addition, lymph node to background contrast in the neck and axilla did not improve on the delayed scan owing to the stable muscle uptake of FDG between 1 and 2 h.

FDG entry into cancer cells is mediated by glucose transporter, and FDG is subsequently phosphorylated by hexokinase. Because of the low de-phosphorylation rate of FDG-6-phosphate, it is trapped in cancer cells and fluorine-18 emits large amounts of positrons from cancer cells. Even after a fall in the blood level of FDG at 1–2 h after injection, most tumours in our study showed increased FDG uptake from 1 to 2 h. This could be achieved only under a very high transport rate and a very low level of free FDG within the cell, which produced a gradient in the level of free FDG (higher outside and lower inside the cell). These conclusions seem to be consistent with the fact that cancer cells have high levels of both glucose transporter and hexokinase [22]. Recent in vitro studies have shown that the activity of glucose transporter, and not that of hexokinase, is the rate-limiting step in FDG uptake by cancer cells [23]. In fact, comparative studies of FDG-PET and histochemical evaluation of resected tumour tissue of breast cancer [24] and lung cancer [25] have shown the presence of a strong correlation between FDG uptake and the level of glucose transporter expression. In the present study, we have shown the advantage of delayed imaging of FDG but did not provide kinetic constants. Further evaluation of kinetic studies would provide direct evidence for the importance of the parameters k_1 and k_3 in the delayed high uptake of FDG by cancer cells and the lower uptake by normal tissue.

We used 3D data acquisition with fast emission scan covering the vertex to the pelvis within 30 min. Most protocols routinely used with 2D imaging take a longer time. This means that whole-body imaging beginning with the pelvis at 60 min post injection may image lung or neck tumour as late as 90 min or even 120 min. Thus the actual imaging time of such tumours is approaching the time point of our late scans, and the tumour images may have the same characteristics as the late images. Attention should be paid to this point in the planning and evaluation of imaging protocols in patients with different tumours.

In applying the delayed imaging protocol, consideration of the sensitivity of the detector of the PET scanner is extremely important. Delayed imaging may suffer from higher noise owing to the radioactivity decay of ^{18}F. The advantage of higher FDG uptake by lesions may be offset by considerably worse statistics, which may be important for small lesions.

FDG imaging at 3 h might be feasible. Lowe et al. [13] and Nakamoto et al. [21] demonstrated that uptake by several lung and pancreatic tumours started to decrease at 3 h. Furthermore, Boemer et al. [17] recommended the use of a 3-h protocol for breast cancer detection. The value of 3-h imaging seems to vary depending on the type of tumour, as well as on the balance between increased tumour uptake and reduced uptake by normal tissue. Imaging at 2 h might be more widely applicable for various types of tumour. In this study, we did not examine the merits of imaging at 3 h and thus further studies are necessary. Our protocol in this study took 1.5 h for imaging, because it was a sequential study at 1 h and 2 h with attenuation correction for research purposes. For routine clinical examination, we propose single time point imaging at 2 h after injection. This method is likely to provide better tumour detectability.

In conclusion, most malignant lesions were easier to detect in images acquired at 2 h than at in images acquired at 1 h owing to increased tumour uptake and decreased normal background. Whole-body FDG-PET imaging for tumour detection should be performed 2 h after injection to obtain more reliable results.

Acknowledgements. We thank the staff of the Cyclotron Radioisotope Center and the Institute of Development, Aging and Cancer, Tohoku University, particularly Mr. Watanuki and Mr. Miyake, for their excellent technical assistance.

This work was supported by Grants-in-Aids No. 12470183 and 11878002 from the Ministry of Education, Science, Sports and Culture, Japan.

References

1. Conti PS, Lilien DL, Hawley K, Keppler J, Grafton ST, Bading JR. PET and [^{18}F]-FDG in oncology: a clinical update. *Nucl Med Biol* 1996; 23:717–735.
2. Kubota K, Matsuzawa T, Fujiwara T, et al. Differential diagnosis of lung tumor with positron emission tomography: a prospective study. *J Nucl Med* 1990; 31:1927–1933.
3. Coleman RE. PET in lung cancer. *J Nucl Med* 1999; 40:814–820.
4. Moog F, Bangerter M, Diederichs CG, et al. Lymphoma: role of whole-body 2-deoxy-2-[F-18]fluoro-D-glucose(FDG) PET in nodal staging. *Radiology* 1997; 203:795–800.
5. Moog F, Bangerter M, Diederichs CG, et al. Extranodal malignant lymphoma: detection with FDG-PET versus CT. *Radiology* 1998; 206:475–481.
6. Wahl RL, Cody RL, Hutchins GD, Mudgett EE. Primary and metastatic breast carcinoma: initial clinical evaluation with PET with the radiolabeled glucose analogue 2-[F-18]-fluoro-2-deoxy-D-glucose. *Radiology* 1991; 179:765–770.
7. Adler LP, Faulhaber PF, Schnur KC, Al-Kasi NL, Shenk RR. Axillary lymph node metastasis: screening with [F-18]2-deoxy-2-fluoro-D-glucose (FDG) PET. *Radiology* 1997; 203:323–327.
8. Reivich M, Alavi A, Wolf A, et al. Glucose metabolic rate kinetic model parameter determination in humans: the lumped constants and rate constants for [^{18}F]fluorodeoxyglucose and [^{11}C]deoxyglucose. *J Cereb Blood Flow Metab* 1985; 5:179–192.
9. Nolop KB, Rhodes CG, Brudin LH, et al. Glucose utilization in vivo by human pulmonary neoplasms. *Cancer* 1987; 60:2682–2689.
10. Lindholm P, Minn H, Leskinen S, Bergman J, Ruotsalainen U, Joensuu H. Influence of the blood glucose concentration on FDG uptake in cancer – a PET study. *J Nucl Med* 1993; 34:1–6.
11. Imran MB, Kubota K, Yamada S, et al. Lesion-to-background ratio in nonattenuation corrected whole-body FDG PET images. *J Nucl Med* 1998; 39:1219–1223.
12. Kubota R, Kubota K, Yamada S, Tada M, Ido T, Tamahashi N. Microautoradiographic study for the differentiation of intratumoral macrophages, granulation tissues and cancer cells by the dynamics of fluorine-18-fluorodeoxyglucose uptake. *J Nucl Med* 1994; 35:104–112.
13. Lowe VJ, Delong DM, Hoffman JM, Coleman RE. Optimum scanning protocol for FDG-PET evaluation of pulmonary malignancy. *J Nucl Med* 1995; 36:883–887.
14. Hamberg LM, Hunter GJ, Alpert NM, Choi NC, Babich JW, Fischman AJ. The dose uptake ratio as index of glucose metabolism: useful parameter or oversimplification? *J Nucl Med* 1994; 35:1308–1312.
15. Hoegerle S, Juengling F, Otte A, Altehoefer C, Moser EA, Nitzsche EU. Combined FDG and [F-18]fluoride whole-body PET: a feasible two-in-one approach to cancer imaging? *Radiology* 1998; 209:253–258.
16. Hustinx R, Smith RJ, Benard F, et al. Dual time point fluorine-18 fluorodeoxyglucose positron emission tomography: a potential method to differentiate malignancy from inflammation and normal tissue in the head and neck. *Eur J Nucl Med* 1999; 26:1345–1348.
17. Boemer AR, Weckesser M, Herzog H, et al. Optimal scan time for fluorine-18 fluorodeoxyglucose positron emission tomography in breast cancer. *Eur J Nucl Med* 1999;26:226–230.
18. Culbert PA, Adam MJ, Hurtado ET, et al. Automated synthesis [^{18}F]FDG using tetrabutylammonium bicarbonate. *Appl Radiat Isot* 1995; 46:887–891.
19. Fujiwara T, Watanuki S, Yamamoto S, et al. Performance evaluation of a large axial field-of-view PET scanner: SET-2400 W. *Ann Nucl Med* 1997; 11:307–313.
20. Kubota K, Matsuzawa T, Ito M, et al. Lung tumor imaging by positron emission tomography using C-11 L-methionine. *J Nucl Med* 1985; 26:37–42.
21. Nakamoto Y, Higashi T, Sakahara H, Tamaki N, Imamura M, Konishi J. Delayed FDG-PET scan for the differentiation between malignant and benign lesions. *J Nucl Med* 1999; 40:247p.
22. Waki A, Fujibayashi Y, Yokoyama A. Recent advances in the analyses of the characteristics of tumors on FDG uptake. *Nucl Med Biol* 1998; 25:589–592.
23. Waki A, Kato H, Yano R, et al. The importance of glucose transport activity as the rate-limiting step of 2-deoxyglucose uptake in tumor cells in vitro. *Nucl Med Biol* 1998; 25: 593–597.
24. Brown RS, Leung JY, Fisher SJ, et al. Intratumoral distribution of tritiated-FDG in breast carcinoma: correlation between Glut-1 expression and FDG uptake. *J Nucl Med* 1996; 37:1042–1047.
25. Brown RS, Leung JY, Kison PV, Zasadny KR, Flint A, Wahl RL. Glucose transporters and FDG uptake in untreated primary human non-small cell lung cancer. *J Nucl Med* 1999; 40:556–565.